

## A Semi-Automated Molecularly Imprinted Polymer Solid-Phase Extraction Method for Catechin Analysis from Jaboticaba (*Plinia* sp.) Peel Extract Samples by UHPLC-DAD

Alessandra T. Cardoso,<sup>a</sup> Rafael O. Martins,<sup>ib</sup><sup>a</sup> Lucas S. Machado,<sup>ib</sup><sup>a</sup> Lucília Kato,<sup>a</sup>  
Rosineide C. Simas,<sup>b</sup> Carmen Lúcia Cardoso<sup>ib</sup><sup>c</sup> and Andréa R. Chaves<sup>\*a</sup>

<sup>a</sup>Instituto de Química, Universidade Federal de Goiás, 74690-900 Goiânia-GO, Brazil

<sup>b</sup>Escola de Engenharia, Universidade Presbiteriana Mackenzie, 01302-907 São Paulo-SP, Brazil

<sup>c</sup>Departamento de Química, Faculdade de Filosofia Ciências e Letras de Ribeirão Preto,  
Universidade de São Paulo, 14040-903 Ribeirão Preto-SP, Brazil

Jaboticaba (*Plinia* sp.), a nutritionally significant Brazilian fruit, is rich in phenolic compounds, such as catechin, known for its biological and pharmaceutical properties. Extracting and studying these compounds is an economic and environmental strategy to fully explore the great potential that these chemical compounds have. Therefore, this study focuses on developing a semi-automated solid-phase extraction method using molecularly imprinted polymer for catechin analysis in jaboticaba peel extracts, coupled with an ultra-high-performance liquid chromatography with a diode array detector. The reported polymer demonstrated superior extractor capacity compared to the non-imprinted polymer. Different extraction parameters were optimized, and the method exhibited a linear range of 10 to 100  $\mu\text{g mL}^{-1}$  for catechin. The obtained precision with the coefficient of variation was below 7.3%, and the limits of quantification and detection were 12.4 and 4.1  $\mu\text{g mL}^{-1}$ , respectively. The developed sorbent maintained analytical performance through approximately 40 injections. Results suggest that the reported method could efficiently extract catechin from jaboticaba peels in less than 10 min, providing a promising tool for the rapid investigation of natural products. This selective and sustainable approach demonstrated here contributes to the economic and environmental aspects of catechin extraction and analysis in jaboticaba fruit.

**Keywords:** condensed tannins, catechin, solid-phase extraction, *Myrciaria* sp., molecularly imprinted polymer

### Introduction

Phenolic compounds are a class of secondary metabolites commonly found in many parts of plants, such as fruits and leaves.<sup>1</sup> These secondary metabolites have meaningful biological functions in the system of the plants, which includes their defense response against a natural enemy. Moreover, these compounds can also be produced by the plant during stressful conditions and are responsible for providing astringency, color, and flavor to their fruits.<sup>2</sup> In addition to their biological functions, phenolic compounds exhibit commercial interest, since they have industrial applications, such as their usage in additives for paints, drugs, food, among others.<sup>3</sup> Consequently, it is economically

relevant to find potential sources of phenolic compounds to achieve higher phenolic levels from unexplored or non-traditional sources including plant or fruit residues.

Jaboticaba (*Plinia* sp.) is a Brazilian native fruit well-known and considered a rich source of phenolic compounds according to the literature.<sup>4</sup> Over the decades, the fruit has been extensively investigated for its biological properties, such as antioxidant activity, antidiabetic, anticancer mechanisms, and preventive mechanisms that inhibit cardiovascular and circulatory diseases.<sup>5</sup> Moreover, the fruit has been also used to treat Alzheimer's disease and improve memory.<sup>6</sup> Furthermore, studies have indicated that the consumption of phenolic compound sources plays an important role in the treatment and prevention of many immunological and circulatory diseases as well as diabetes and obesity.<sup>7</sup> In Brazil, the jaboticaba pulp is mainly used in the manufacturing of sweets, liqueurs, and

\*e-mail: andrea\_chaves@ufg.br

Editor handled this article: Hector Henrique F. Koolen (Associate)



jellies, while the peel is normally discarded as a production residue, being commonly incinerated in order to provide energy generation.<sup>8</sup> Studies<sup>9,10</sup> have shown that phenolic compounds, such as catechin and epicatechin gallate isolated from jaboticaba exhibited antimicrobial activity, and presented antidiabetic effects with a powerful inhibition of  $\alpha$ -glucosidase and  $\alpha$ -amylase.

Considering the chemical proprieties of phenolic compounds and regarding their economic value, it is hugely necessary to propose an efficient analytical method that is capable of determining these analytes in natural sources, for instance, ultra-high performance liquid chromatography coupled with a diode array detector (UHPLC-DAD) has been a widely used separation technique for this purpose.<sup>11</sup> Nonetheless, the presence of several other substances, such as pigments and sugars in the jaboticaba extract matrix, represents a formidable challenge for the evaluation by analytical instrumentations, such as UHPLC-DAD.<sup>12</sup> Hence, the application of an extraction technique that promotes the cleanup of the matrix before the separation while also maintaining the integrity of the analyte is always required. Therefore, automated, and semi-automated extraction techniques have shown great achievements in the literature, especially with miniaturized systems, that use a minimum volume of organic solvents, extraction sorbents, and sample volume required. Such advantages decrease the environmental impact and provide higher analytical throughput of the method. Moreover, the coupling of the extraction step directly to the separation system reduces the analytical errors from sample handling and contributes to the improvement of the analytical performance of the method, once there is no sample lost during the analytical procedure.<sup>13</sup>

One of the main aspects that define the success of an extraction method is the interaction between the sorbent and the analyte. A class of polymers commonly known as molecularly imprinted polymer (MIP) has been successfully used in several extraction techniques, as it presents higher selectivity to the target analytes. This class of polymers uses a template molecule during its synthesis creating specific recognizable sites that are later used for the specific binding with the target analyte.<sup>14</sup> The use of MIP to perform the extraction of phenolic compounds from Brazilian natural sources is already described in the literature, mostly as sorbent for conventional sample preparation methods, such as solid-phase extraction (SPE).<sup>14</sup> However, to the best of our knowledge, this is the first time that a semi-automated solid phase extraction method using MIP as a sorbent phase in the extraction device for the determination of phenolic compounds from the jaboticaba peel extract has been reported. Hence, this study presents a semi-automated methodology using MIP as a sorbent in the extraction

column coupled with UHPLC-DAD to promote the cleanup and enrichment of phenolic compounds present in the jaboticaba peel (*Plinia* sp.).

## Experimental

### Reagents and solvents

Acetonitrile, acetone, and methanol high-performance liquid chromatography (HPLC) grade were purchased from Tedia (Fairfield, CT, USA). Ethanol 92.8% was acquired from Super Sol (Uberlândia, MG, Brazil). Silica gel was purchased from Macherey-Nagel, Germany, while the water was ultra-purified in MS2000 WFI equipment (Gehaka, SP, Brazil). Formic acid (95%), ammonium hydroxide (30%), tetraethoxysilane (TEOS) (98%), 3-aminopropyltriethoxysilane (APTES) (99%), and (+)-catechin standard (98%) were obtained from Sigma-Aldrich (St. Louis, MO, USA). Individual stock solutions of catechin were prepared at a final concentration of 1 mg mL<sup>-1</sup> in methanol and stored at -4 °C in an amber flask. The catechin solution was used during method optimization.

### Equipment

Rotary evaporator from Biovera (Rio de Janeiro, Brazil), SpeedVac from Thermo Scientific (Tokyo, Japan), Fourier transform infrared (FTIR) PerkinElmer Spectrum 400 model (Waltham, Massachusetts), scanning electron microscopy (SEM) using a Jeol JSM-6610 model, equipped with energy-dispersive X-ray spectroscopy (EDS) from Thermo Scientific (Tokyo, Japan), transmission electron microscopy (TEM) with a Jeol JEM-20100 model, equipped with EDS from Thermo Scientific (Tokyo, Japan), X-ray diffraction (XDR) using a Shimadzu diffractometer XRD-6000 model (Kyoto, Japan), thermogravimetry (TGA) analysis in the Netzsch STA 449 model (Newcastle, USA). Micrometric ASAP 2020 Plus version 1.03 (Norcross, USA), UHPLC 1260 Infinity II, equipped with 1260 Infinity II Multisampler, and DAD detector from Agilent Technologies (Santa Clara, USA), Q Exactive hybrid Quadrupole-Orbitrap from Thermo Scientific (Tokyo, Japan) were used.

### Jaboticaba peel samples

Jaboticaba samples were obtained at Fazenda Jaboticabal, located in the city of Hidrolândia, Brazil (16°55'32.35" S, and 49°21'39.76" W). The use of jaboticaba was registered on SisGen/Brazil, protocol number A43ECB6. The samples were stored in plastic

bags under a refrigeration system (18 °C). The peels were manually separated from the pulp, and completely dried at a temperature of 35 °C for three days, and then crushed. A total of 25 g from the powder jaboticaba peel was submitted to Soxhlet extraction using 500 mL of ultra-purified water, under a temperature of 100 °C for 6 h of extraction. The obtained extract was filtered and concentrated in a rotary evaporator, and subsequently dried in a SpeedVac instrument. The dried extract was kept under refrigeration (−4 °C), and 1 mg was resuspended in 1 mL of water/acetonitrile/formic acid (85:15:0.1 v/v), with the mixture at a final concentration of 1 mg mL<sup>−1</sup> (crude extract).

#### Synthesis of the molecularly imprinted polymer and non-imprinted polymer

The synthesis of the MIP was performed considering the protocol described by Martins *et al.*<sup>14</sup> For the MIP synthesis, 0.5 g of silica was mixed with 160 mL of ultrapure water, 100 mL of methanol (porogen solvent), and 20 mL of ammonium hydroxide (catalyzer). The solution was then reacted with 8 mL of TEOS (crosslinker), 1 mL of 3-aminopropyl-triethoxysilane-APTES (functional monomer), and 5 mL of a catechin standard solution (1 mg mL<sup>−1</sup>) as the template molecule.

After homogenization, the reaction medium was subject to stirring for 24 h at 25 °C. The suspension was filtered and dried in an oven system (50 °C) for 24 h. The dried polymers were submitted to the Soxhlet system for 24 h in ethanol for template removal. The washing step was repeated with an acetone for another 3 h for template and unbound reagents synthesis residues removal. To compare the extraction capacity of the developed MIP, a non-imprinted polymer (NIP) synthesis was performed using the described methodology described for MIP without the addition of the template molecule (catechin) in the synthesis medium.

#### Characterization of the MIP and NIP

All the synthesized polymers were subjected to characterization procedures by physical-chemical techniques. Furthermore, FTIR spectroscopy analysis was performed in the range of 450 to 4500 cm<sup>−1</sup>. The morphology of the materials was investigated by SEM analysis, at a magnitude of 15,000×, and an accelerating potential of 7 kV, and by TEM analysis at a wavelength of 1 μm and 200 nm.

The crystallinity degree information of the MIP and NIP, XDR was obtained by using a voltage of 40 kV, a current of 30 mA, a scanning speed of 4° s<sup>−1</sup>, and a Cu K radiation detection range ( $\lambda = 1.54 \text{ \AA}$ ) of 10–80 °C. The

thermal stability of the polymers was evaluated by a TGA analysis. To perform TGA assays, a mass of ±7.5 mg of MIP and NIP samples were placed in an alumina crucible and heated from 25 to 1000 °C, at a scan rate of 10 °C min<sup>−1</sup> and a nitrogen gas flow rate at 50 mL min<sup>−1</sup>. The surface area, pore size, and pore volume of the MIP were determined from nitrogen adsorption using a Micrometrics ASAP 2020 Plus Version 1.03 (Norcross, USA), with approximately 300 mg of polymers, heated at 350 °C for 10 h, then subject to nitrogen gas adsorption. The Barrett-Joyner-Halenda (BJH) model was applied to determine the size and volume of the pores, while the Brunauer-Emmett-Teller (BET) model was used for the determination of the surface area.

#### Preparation of packed capillaries and method optimization

Capillaries were prepared with 100 mm × 0.25 mm internal diameter (i.d.) polyether ether ketone (PEEK) tubes, 1/16-in stainless steel long fittings with front and back ferrules, 1/16-in zero-volume union fitted, and 10 μm stainless steel frit from Agilent Technologies (Santa Clara, USA). Based on capillary geometry and dimensions, the estimated volume was 20 μL. The MIP and NIP sorbents (10 mg) were slurred in methanol, homogenized, and left to rest for 24 h at room temperature (25 °C). Subsequently, the solution was packed into the PEEK tubing by the slurry packing method. After the packing step, the columns were monitored in a UHPLC-DAD system with an isocratic flow of methanol (0.05 mL min<sup>−1</sup>), until reaching constant pressure and a totally packed column. Afterward, the capillary columns were conditioned with methanol (100% v/v) for 1 h, followed by another 1 h with methanol/formic acid (99.9:0.1% v/v) before the use.

For the semi-automated solid-phase extraction with molecularly imprinted polymer (semi-automated MIP-SPE) method, the conditioning step was performed with water/acetonitrile (85:15% v/v) at 20 μL min<sup>−1</sup> for packed capillary. During the extraction procedure, the samples were injected (40 μL) directly into the MIP capillary column and after 2 min of extraction, a fraction (100 μL) was collected, dried, and resuspended in the same volume in proportion to the mobile phase for subsequent separation in an analytical column. For the chromatographic separation of real samples, an analytical column was used.

The diameter of the capillary column was also evaluated to provide the best response for the proposed methodology. For this, a capillary of a 100 mm × 0.13 mm i.d. dimension was prepared with the MIP phase under the same conditions as the 0.25 i.d. capillary. A catechin standard at 50 μg mL<sup>−1</sup> was utilized for the injections and the evaluation of extraction efficiency.

The optimization method was performed by the univariate evaluation of the main analytical parameters involved during the extraction procedure using a standard catechin solution at a final concentration of 50  $\mu\text{g mL}^{-1}$ . The evaluation of the extraction condition included the following parameters: injection volume (5, 10, 20, 30, 40, 50, 75, and 100  $\mu\text{L}$ ), loading flow (15, 20, 25, 50, and 75  $\mu\text{L min}^{-1}$ ), and the relationship between the flow rate and back pressure of the MIP and NIP capillaries, both at the same flow.

#### Instrumental conditions

The semi-automated MIP-SPE method consisted of an extraction PEEK capillary column (100 mm  $\times$  0.25 mm i.d.) fixed after the injection loop site of the equipment and was carried out in a UHPLC 1260 Infinity II, equipped with 1260 Infinity II Multisampler, and DAD detector from Agilent Technologies (Santa Clara, USA). Chromatographic separation was performed in an analytical column model called ZORBAX Eclipse XDB-C18 1PK (4.6  $\times$  50 mm  $\times$  1.8  $\mu\text{m}$  particle size), from Agilent Technologies (Santa Clara, USA) under the following conditions: column temperature, 25  $^{\circ}\text{C}$ ; flow rate, 300  $\mu\text{L min}^{-1}$ ; injection volume, 10  $\mu\text{L}$  and mobile phase constituted by A: (water/formic acid, 99:0.1 v/v) and B: (acetonitrile/formic acid 99:0.1 v/v), in isocratic mode (85% A:15% B) for 20 min with the monitored wavelength at 280 nm.

After the optimization step, figures of merit were evaluated, and the catechin molecule confirmation in the real samples was performed in a Q Exactive hybrid Quadrupole-Orbitrap from Thermo Scientific (Tokyo, Japan) coupled to the UHPLC system aiming to verify the mass spectrum (MS) profile of the (i) crude sample and, (ii) the sample after extraction by the developed online method. The MS conditions applied were: electrospray ionization applying negative ion mode (ESI $^{-}$ ) tandem mass spectrometry (MS/MS) for monitoring the ion at  $289.1 \pm 0.45 m/z$ ; a mass range of 150 to 300  $m/z$ ; maximum injection time of 50 ms; nitrogen flow of 10 (arbitrary units, a.u.); the auxiliary gas flow of 5 a.u.; spray voltage of 3.10 kV; and capillary temperature of 320  $^{\circ}\text{C}$ . The spectra were processed using the software Xcalibur Analysis (version 2.0, Service Release 2, Thermo Electron Corporation).

#### Evaluation of MIP extraction capacity

The extraction capacity of the MIP phase was evaluated by comparing the chromatogram areas obtained with catechin solution (50  $\mu\text{g mL}^{-1}$ ) injections into the MIP

capillary column compared to those packed with the NIP phase ( $n = 3$ ).

#### Analytical figures of merit

To evaluate the parameters of the linearity, repeatability, and reuse capacity of the capillary, the International Conference on Harmonisation (ICH) guidelines were used.<sup>15</sup> The developed methodology was investigated considering the calibration curves constructed in the range of 10  $\mu\text{g mL}^{-1}$  to 100  $\mu\text{g mL}^{-1}$  and the limit of detection (LOD) and limit of quantification (LOQ) were obtained by equations 1 and 2.<sup>16</sup>

$$\text{LOD} = \frac{3.3 \times \text{sB}}{m} \quad (1)$$

$$\text{LOQ} = \frac{10.0 \times \text{sB}}{m} \quad (2)$$

where sB is the standard deviation of 10 blank measurements, and m is the slope of the calibration curve.

Precision was expressed in terms of the repeatability of the MIP capillaries using three capillaries at the same dimension and extraction phase mass to perform the extraction of the standard solution of catechin. Moreover, the precision was measured by a coefficient of variation (CV, in percentage). To determine the CV, three concentration levels were considered, encompassing low, medium, and high concentrations (30, 50, and 100  $\mu\text{g mL}^{-1}$ ) for MIP and NIP columns in the triplicate assay ( $n = 3$ ), and the intra-day precision was determined according to equation 3:

$$\text{CV}(\%) = \left( \frac{s}{\bar{x}} \right) \times 100 \quad (3)$$

where s is the standard deviation between replicates and  $\bar{x}$  is the average of the injections.

The reusability of the MIP capillary column was performed by assessing the relative standard deviation (RSD) between the injections of the catechin standard solution, in the same chromatographic conditions. As an acceptability criterion, the following values were considered: CV < 15% and RSD < 20%.<sup>17,18</sup> The carryover was assessed by comparing the chromatogram areas (standard solution at 100  $\mu\text{g mL}^{-1}$ ) with the injection of a blank sample (methanol solution) in the extractor column after the chromatography analysis. Lastly, the enrichment factor of the semi-automated MIP-SPE method was evaluated, comparing the areas of the same catechin standard (100  $\mu\text{g mL}^{-1}$ )



extracted by the MIP column and injected directly into the chromatographic system, without going through the extraction procedure, in triplicate.

## Results and Discussion

### MIP and NIP characterization

The selection of catechin as the template molecule for MIP synthesis was deliberate, driven by its status as a well-known phenolic compound abundant in jaboticaba and of commercial interest.<sup>14</sup> Moreover, many literature reports<sup>9,10</sup> indicate its presence in jaboticaba peels and the relationship with a bioactive potential originating from the catechin molecule. In terms of structural evidence, the catechin skeleton resembles those other classes of bioactive phenolic compounds, such as condensed tannins. This highlights its potential as an approach for synthesizing MIPs, particularly for the extraction of catechin derivatives.<sup>14</sup>

SEM images of MIP and NIP-developed polymers were performed to investigate polymer morphology (see Figure 1A). According to Figure 1A, both the MIP and NIP presented morphological characteristics of regular solids with spheric and cluster particles. Regarding the morphological differences between the MIP and the NIP, it is noted that the spacings between the particles are more pronounced in the MIP. The presence of cavities in MIP particles is a desirable characteristic for solid sorbents due to the better elution of the loading flow through the SPE column, reducing the pressure in the system and the carryover effect between the analysis. As a consequence, allowing it to be reused. Aiming to complement the morphological MIP and NIP evaluation, TEM analysis was carried out. According to the obtained results (Figure 1B), the MIP presented more microparticle clusters than the NIP. Besides, the darker color particles (mainly the NIP particles) could be attributed to higher particle density, which can retain the electrons transmitted in the TEM analysis.<sup>19</sup> The NIP particles ultimately exhibited less porosity and presented higher density, corroborating with the SEM results.

The literature<sup>19</sup> indicates that MIP polymers predominantly exhibit amorphous characteristics throughout their structure. Therefore, to verify the crystallinity degree of these sorbents, an XDR analysis was performed (Figure 1C). As shown in Figure 1C, the MIP and NIP diffractograms indicated that both polymers had similar profiles. In polymeric materials, there are ordered and disordered regions in the same material, contrary to the slightly crystalline materials that usually present well-defined patterns.<sup>20</sup> According to Figure 1D, the peak around  $22.6^\circ$  is characteristic of amorphous solids and does not

refer to precise and well-defined distances. Accordingly, for ordered and partially crystalline regions, TEM micrographs present darker regions in some particles.

The information about the functional groups present in the synthesized polymers was obtained by FTIR analysis. The obtained spectra are presented in Figure 1D. The results indicate that both profile spectra of the polymers were very similar. The APTES was used as a functional monomer for the MIP and NIP syntheses and has in its structure a primary amine group ( $\text{NH}_2$ ) that presents bending with light absorption at approximately  $1640\text{ cm}^{-1}$ . The stretching band at  $3440\text{ cm}^{-1}$  refers to the hydroxyl group (OH) adsorption, on account of the strength of the hydrogen bond.<sup>21</sup> The intense band at  $1078\text{ cm}^{-1}$  represents a vibration of the Si–O–Si bond, from the silica used for the synthesis of the polymer.<sup>22</sup>

As indicated by the TGA results (Figure 1E), the MIP and NIP polymers did not display any decomposition curves, only a relatively small constant weight loss at the end of the process (less than 20%). The initial weight loss of two polymers (until  $100^\circ\text{C}$ ) may be associated with the dehydration process of the methanol and water, used as solvents in the synthesis. Between  $500$  and  $700^\circ\text{C}$ , the loss of mass is observed as a result of reagent residues and dihydroxylation of the polymers that are present, respectively. The MIP is commonly more thermally stable than the NIP since the functional monomers-template interaction during the polymerization process makes the MIP less likely to lose weight.<sup>23</sup>

Finally, the surface area, pore volume, and average pore diameter of MIP and NIP were measured using BET and BJH methods, with the obtained results displayed in Table S1 (Supplementary Information (SI) section). As the literature reports,<sup>24</sup> the surface area of MIP is generally greater than the NIP, once the porosity could be influenced by the presence of the template in the polymerization process. According to Middelcer *et al.*<sup>25</sup> the size, morphology, and porosity of MIP particles play an important role in the interaction with the target analyte. It is expected that the larger the surface area is, the greater the selectivity of the target rebinding is. The morphology results acquired in this study indicated that both polymers had a mesopore characteristic, although studies indicate that polymers usually used for extraction systems present sizes between  $10\text{--}18\text{ nm}$ .<sup>26,27</sup> This study obtained volume values for MIP of  $0.4056\text{ cm}^3\text{ g}^{-1}$  and pore size of  $17.26\text{ cm}^3\text{ g}^{-1}$  which are compatible values obtained by Martins *et al.*<sup>14</sup> which indicates efficiency in the use of synthesized MIP in the sample preparation process. Moreover, the acquired results favorably point out the application of the synthesized MIP as an extraction phase.<sup>28,29</sup>

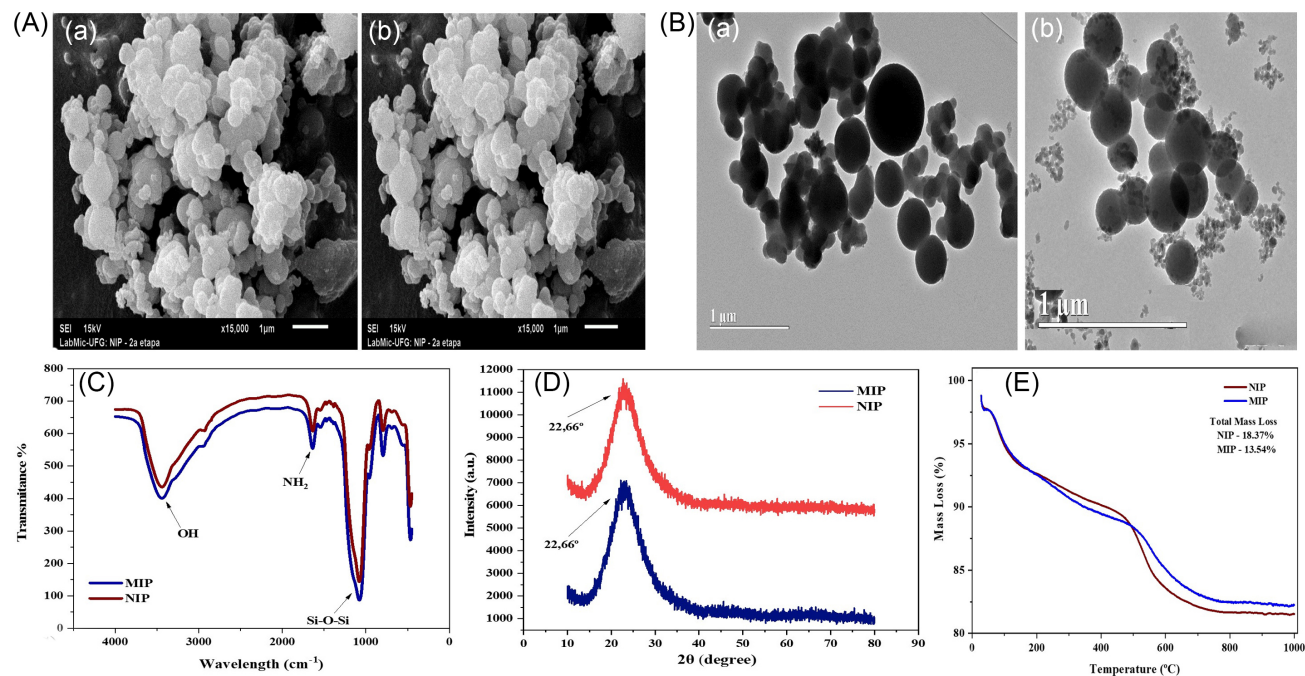


**Figure 1.** (A) Scanning electron micrograph of MIP (a) and NIP (b). (B) Transmission electron microscopy of MIP (a) and NIP (b); FTIR (KBr) spectra obtained from MIP and NIP (C); diffractograms of MIP and NIP (D); TGA curves (E).

### Evaluation of MIP extraction capacity

The extraction capacity was evaluated considering the ability of the MIP sorbent to determine the catechin. To this aim, the obtained peak area results were compared with those obtained by the NIP column phase (Figure 2). As stated by the data in Figure 2, it is possible to note that the MIP presented a peak area about 70% higher than the NIP. This gives greater recognition of the catechin and enrichment abilities. This result was already expected, as the MIP sorbent phase has specific binding sites for catechin molecule recognition, in addition to its surface area ( $93.9929 \text{ m}^2 \text{ g}^{-1}$ ) being relatively larger than that of

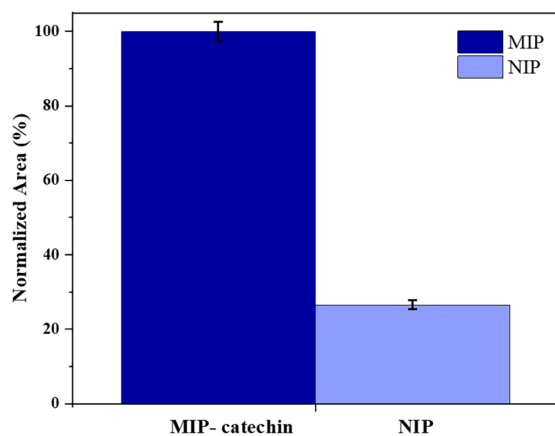


**Figure 2.** MIP and NIP extraction capacity for the standard catechin solution ( $n = 3$ ,  $50 \mu\text{g mL}^{-1}$ ).

NIP ( $88.2622 \text{ m}^2 \text{ g}^{-1}$ ), which increases the chances of the sorbent having greater capacity to rebind the analyte.<sup>25</sup>

### Optimization of the method variables

For method development, 100 mm of a capillary PEEK column was used as support for the MIP extraction particles, as described in the Experimental section. First, the column containing the polymer sorbent was conditioned with the mobile phase. Moreover, some important analytical parameters were studied, these parameters include the size (0.13 and 0.25 mm) of capillary diameter, the analyte retention time and pressure resistance in order to achieve the best extraction conditions. Regarding the phase applicability, the obtained results for the 0.13 mm diameter columns were consistent, with the intensity and retention time (13.5 min) showing strong retention with the analyte (Figure S1 see SI section). However, when it comes to extractor columns used in automated or semi-automated methods, it is important to ensure the support of the pressure exerted by the system in which the analysis is carried out.

Furthermore, the use of columns of 0.13 mm diameter became unfeasible after three injections, especially since the high equipment pressure reduced the useful life of the capillaries. Consequently, subsequent investigations were conducted using a column featuring a 0.25 mm diameter, showcasing a shorter retention time (2.2 min) and superior mechanical strength, as evidenced by the reusability of the column (Figure S2, SI section). The decrease in catechin

retention time observed in the 0.25 mm column, as opposed to the 0.13 mm column, can primarily be attributed to the expanded pathways available for the analyte to traverse. This phenomenon aligns with Van Deenter's theory, given the structure of the applied column, which comprises a packed phase.

The injection volume, ranging from 5 to 100  $\mu\text{L}$ , was also evaluated. The results are presented in Figure 3 as the percentage of the normalized area. As depicted in Figure 3a, the peak areas exhibit a discernible augmentation corresponding to the increase in injection volume. Nevertheless, the asymmetric factor of the catechin peak is one of the parameters that need to be evaluated for a satisfactory chromatographic extraction method. Table 1 shows the ratio of the asymmetry factor for each evaluated injection volume. The literature<sup>30</sup> reports that the cause of chromatographic peak asymmetry is mainly linked to column overloading, and acceptable values for packed columns range from 0.75 to 1.25. Even though in the present study the capillary was designed for only catechin derivate compounds extraction, overloading the column can reduce the extraction efficiency and the lifetime of the capillary.

**Table 1.** Asymmetry factors for each injection volume evaluated and loading flow ( $n = 3$ )

Injection volume / $\mu\text{L}$	Asymmetry factor	Mobile phase flow / ( $\mu\text{L min}^{-1}$ )	Asymmetry factor
5	1.61	15	1.16
10	1.45	20	1.09
20	1.21	25	1.23
30	1.28	50	1.28
40	0.93	75	0.92
50	0.84	–	–
75	0.99	–	–
100	0.87	–	–

Therefore, although the volume of 75  $\mu\text{L}$  is within the acceptable range of asymmetric value (0.99), this volume resulted in a carryover effect, thus causing the reduction of the column reusability. For this reason, the injection volume of 40  $\mu\text{L}$  was chosen as the optimum condition for further assays, as it presents an asymmetry value closest to 1 (Table 1).

The loading flow was evaluated considering a range from 15 to 75  $\mu\text{L min}^{-1}$  using the extraction condition described in the Experimental section. The main findings demonstrated that using a lower loading flow resulted in deformation on the chromatographic peak, likely compromising the chromatographic resolution and insufficient desorption of the analyte in the MIP phase.

On the other hand, the use of higher flow rates caused a reduction in the retention time, which could lead to a coelution of catechin with the interfering compounds of the real matrix (jaboticaba powder extracts). Moreover, such an extraction condition could also reduce the efficiency of MIP in providing adequate binding with the target analyte since the interaction between the sorbent and the analyte phase tends to decrease in high-flow conditions, thus resulting in a shorter retention time and coelutions. The corresponding figure with these results can be found in the SI section (Figure S3). Concerning the best loading flow condition, the evaluation also considered the asymmetry factor results obtained in Table 1. In Table 1 the loading flow of 20  $\mu\text{L min}^{-1}$  presented a better asymmetry range, and the same flow contributed to reducing residue generation. This is especially crucial to adopt green analytical strategies that ensure minimal use of organic solvents and reduced waste generation. Through the adoption of these practices, this study aligns with well-established green analytical principles.

The relationship between the flow rate and back pressure of the system using MIP and NIP capillaries was evaluated, and the results are presented in Figure 3b. According to them, the system pressure for both columns increased with the flow rate. Comparing the pressure on the two extraction columns, the NIP phase exhibited higher pressure. As evident from Table S1, the NIP exhibits smaller volume and pore size values compared to the MIP. This characteristic complicates the elution of the loading flow, leading to increased back pressure within the column. Besides, as demonstrated by TEM and SEM analysis, NIP particles are less porous and denser than those in MIP, which contributes to an increased pressure in the separation system. Thus, the volume of 20  $\mu\text{L min}^{-1}$  was used in all subsequent assays to the figures of merit of the developed methodology. According to Li *et al.*<sup>31</sup> a porous surface on the polymer facilitates the transfer of the analyte to the loading flow. However, despite this difference, the results indicated that the two developed columns exhibited adequate performance in terms of pressure resistance, as demonstrated in Figure 3.

#### Analytical method performance

The method showed linearity with coefficient of determination ( $R^2$ ) > 0.997 for catechin in the range of 10 to 100  $\mu\text{g mL}^{-1}$  and the LOD and LOQ were determined to be 4.1 and 12.4  $\mu\text{g mL}^{-1}$ , respectively. Table 2 presents the results of the precision assays, performed in three columns packed with MIP-catechin, using three concentration levels (30, 50, and 100  $\mu\text{g mL}^{-1}$ ) and the

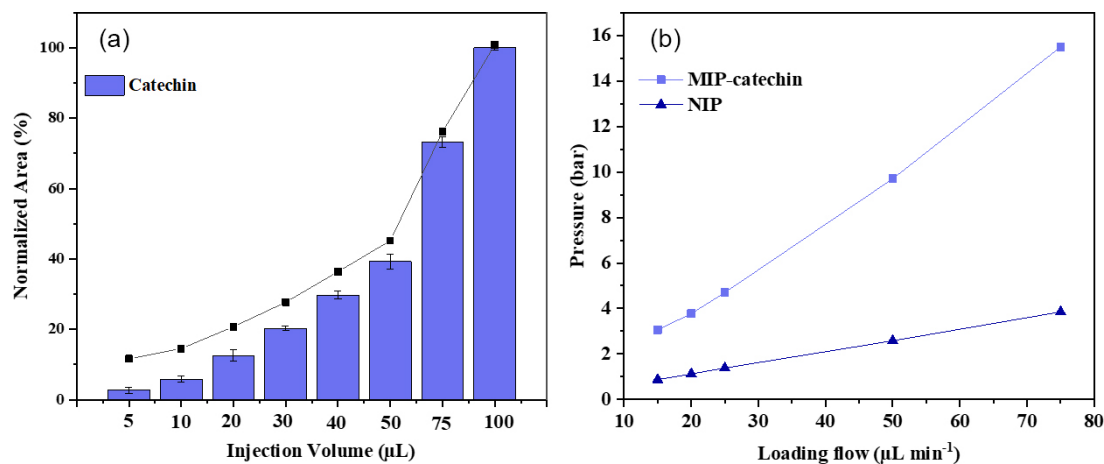


**Figure 3.** Relationship between the evaluated injection volume ( $\mu\text{L}$ ) and the normalized peak area ( $n = 3$ ) (a). Relationship between mobile phase flow ( $\mu\text{L min}^{-1}$ ) and MIP and NIP pressure levels in capillaries (b).

enrichment factor, based on the comparison between the areas of the chromatograms of the solution of the catechin standard subjected to extraction with the MIP capillary, and the standard solution at the same concentration without extraction, injected directly. The results contain values that are less than 7.3%, with a coefficient of variation of  $< 15\%$ , which is acceptable according to the regulatory agencies for analytical methods.<sup>14</sup> Furthermore, MIP presented an enrichment factor of 9.59, considering in this case the potential for excluding sample interferences and the gain in signal intensity from the developed MIP.

**Table 2.** Repeatability for MIP columns at low, medium, and high concentrations expressed in CV for the catechin solution and enrichment factor evaluated at  $100 \mu\text{g mL}^{-1}$

Parameter	Concentration		
	$30.0 \mu\text{g mL}^{-1}$	$50.0 \mu\text{g mL}^{-1}$	$100.0 \mu\text{g mL}^{-1}$
Repeatability (CV) / %	3.2	7.3	2.6
Enrichment factor	–	–	9.59

CV: coefficient of variation.

To verify the reusability of the developed column, a total of 40 injections were performed using the catechin standard solution ( $50 \mu\text{g mL}^{-1}$ ), obtaining a relative standard deviation of 3.83% in terms of peak area variation of the chromatograms. This value suggests that the MIP column could be reused multiple times, at least 40 times, with a minimum reduction of the analyte extraction efficiency. Finally, carryover was evaluated (Figure S4, see SI section). As can be observed in Figure S4, the chromatogram obtained by the solvent in the MIP-catechin column does not present peaks at the same analyte retention time, even after an extraction procedure with the catechin standard at a high concentration level, which indicates that the analyte

was completely desorbed from the extractor phase, leaving no residue.

#### Phenolic content in jaboticaba peel extracts

The jaboticaba peel extract samples were submitted to the developed and optimized online microextraction method. The extracts were resuspended in water/acetonitrile/formic acid (85:15:0.1 v/v) at the final crude extract concentration of  $1 \text{ mg mL}^{-1}$  and injected into the MIP and NIP columns to compare the extraction efficiency purposes. The chromatograms for the MIP and NIP columns, showcasing the separation in an analytical column, are illustrated in Figures S5 and S6 (see SI section). It is crucial to emphasize that the aqueous extracts were collected and resuspended in accordance with the mobile phase for the separation, as detailed in the Experimental section. Moreover, the aqueous extract represents a minimally manipulated sample, involving no addition of organic solvents or solid support-only water and temperature were employed.

In Figure S5, it is possible to observe that in the obtained chromatographic peaks for catechin derivatives, both the MIP and NIP columns showed the same retention time as the standard, 3.8 min (Figure S6). Even so, the MIP column exhibited a higher catechin signal, with a higher peak area which suggests the enrichment of the target analyte. According to the obtained chromatograms, the MIP column also showed better potential for the elimination of the interfering compounds present in the matrix.

Aiming to verify the phenolic compound identity in real jaboticaba peel sample aqueous extracts, MS analysis was performed for (i) extract after semi-automated extraction and (ii) crude extract followed by chromatographic separation procedure. For this purpose, the negative



ionization mode was used and a mass ( $m/z$ ) of 289.07 was monitored for both samples. The obtained spectra are shown in Figures 4a–4b. Figure 4a presents a peak of  $m/z$  289.0781, characteristic of the catechin molecule in the jaboticaba peel samples extracted with the MIP column, whereas in the crude sample at the same analytical analysis condition (Figure 4b), only by zooming in was it possible to see the catechin mass charge. This result shows that the MIP column was successfully applied to the extract catechin and eliminated the interferences that could suppress the analyte signal, which is usually a problem for natural product extracts. The signal intensity for the semi-automated MIP-SPE extracted fraction was relatively higher when compared to the analysis of the crude sample, which was expected since the crude extract demonstrates a greater complexity signal of the compound, which may be due to an ion suppression signal in the mass spectra.

In order to validate the identity of the catechin-derived molecule extracted from the jaboticaba peel sample, a tandem MS/MS analysis was performed (Figure S7, SI section). The spectra in Figure S7 present two characteristic ions of the (epi)catechin molecule: the ions of  $m/z$  205 (indicating the loss of  $C_4H_4O_2$ ) and  $m/z$  245 (indicating the loss of  $CO_2$ ). The confirmation of such fragmentation ions can also be seen in Figure S8. Martins *et al.*<sup>32</sup> found the same mass/charge ratio values in the spectra obtained for açai (*Euterpe oleracea* Mart.) extracts referring to the catechin epimer. Then, from the fragmentation route, it was possible to confirm that the compound observed at the same retention time as the standard solution in Figure S6 was (epi)catechin, a

derivative of the catechin molecule. This outcome indicated that the developed MIP phase was highly selective not only for catechin but for its derivatives, being selectivity for this class of phenolic compounds. According to the obtained results in this study, the MIP extraction phase could improve the analytical performance of the method by the capacity to bind with phenolic compounds and by removing the interfering compounds in real samples.

Moreover, the application of the online analytical method was simple, fast ( $< 10$  min), and with lower sorbent (10 mg) and solvent ( $20 \mu\text{L min}^{-1}$ ) consumption when compared to other conventional, completely offline, and miniaturized extraction methods used for phenolic compound extraction (Table 3). At a laboratory scale, this would improve the analytical frequency for the routine analysis of products containing catechins and flavonoids.

## Conclusions

In this study, a semi-automated MIP-SPE method using MIP as the extraction phase was reported for the catechin and its derivatives in jaboticaba peel powder for the first time. For this purpose, MIP was synthesized using the catechin molecule as a template and applied to the capillary column. The MIP and NIP were subject to physical-chemical characterization, in which the morphological differences between the polymers were observed, specifically since the MIP polymer presented a more porous morphology and greater pore size. According to the method optimization results, the best condition of the online analyses was obtained using a mobile phase

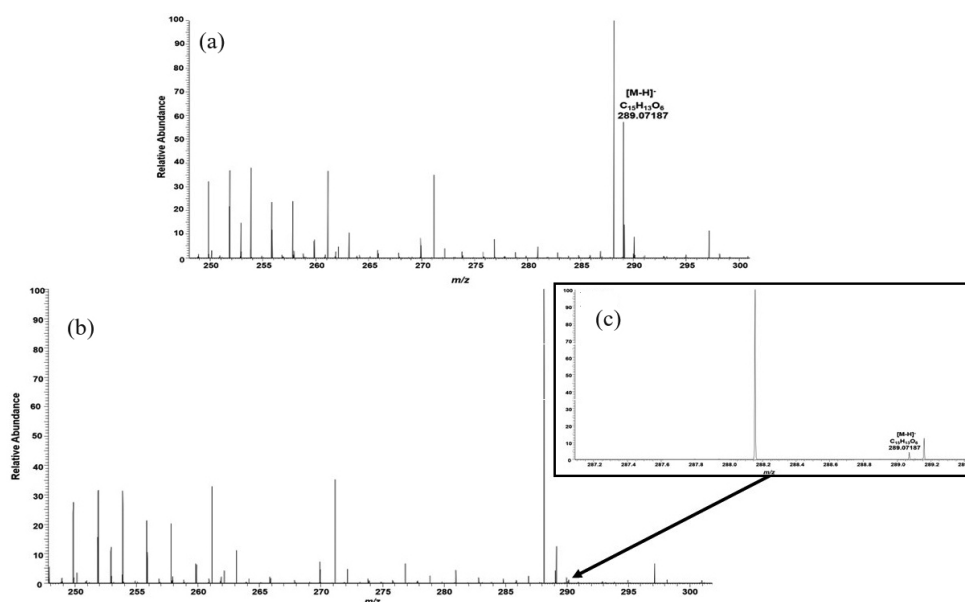


**Figure 4.** (a) ESI ( $-$ ) Orbitrap-MS mass spectrum of the jaboticaba peel matrix extracted with the MIP column for the catechin of  $m/z$  289.07181. (b) ESI ( $-$ ) Orbitrap-MS mass spectrum of the crude jaboticaba peel matrix. (c) Zoom into the peak region of the catechin present in the crude extract fraction.

**Table 3.** Some extraction methods used to extract flavonoids

Analyte	Sample	Extraction method	Amount solvent (elution)	Amount sorbent	Extraction time / min	LOQ	Reference
Quercetin, luteolin, oleuropein vanillic acid	olive oil	SPE	10 mL	200-500 mg	10	5.13 mg L <sup>-1</sup> to 6.33 mg L <sup>-1</sup>	33
Catechin	<i>Anadenanthera macrocarpa</i> , <i>Myrciaria jaboticaba</i> , <i>Spondias tuberosa</i>	MISPE	3 mL	2 g	5	40 mg L <sup>-1</sup>	14
Flavonoids	<i>Citrus limon</i> L.	PLE-SPE	25 mL	500 mg	90	–	34
Canolol, phenolic acids, phenolic alcohols, tyrosol, vanillin	vegetable oils	SPE	3 mL	60 mg	–	0.006 µg kg <sup>-1</sup> to 0.300 µg kg <sup>-1</sup>	35
Coumarins	wine samples	pipette tip	1.5 mL	20 mg	< 10	–	36
Coumarins	wine samples	MISPE	5 mL	0.1 g	15-20	0.3 µg mL <sup>-1</sup> to 12.0 µg mL <sup>-1</sup>	36
Coumarins	wine samples	batch extraction	3 mL	0.2 g	90	–	36
Rosmarinic acid	<i>Rosmarinus officinalis</i>	MISPE	2 mL	40 mg	–	6.09 µg mL <sup>-1</sup>	37
Quercetin	<i>Allium cepa</i> L.	MISPE	9 mL	100 mg	–	–	38
Catechin	jaboticaba peel	semi-automated MIP-SPE	20 µL min <sup>-1</sup>	10 mg	2	12.4 µg mL <sup>-1</sup>	this study

LOQ: limit of quantification; SPE: solid-phase extraction; MISPE: molecularly imprinted solid-phase extraction; PLE-SPE: pressurized liquid extraction and solid-phase extraction; MIP-SPE: solid-phase extraction with molecularly imprinted polymer.

flow of 20 µL min<sup>-1</sup> and a sample injection volume of 40 µL. The method performance was evaluated, and the extraction capacity of the developed MIP for catechin showed coefficients of variation ranging from 2.6 to 7.3% as well as an enrichment factor of 9.59. The enrichment factor associated with the interferent elimination capacity of the developed MIP phase conveyed the potential of the developed methodology to be employed with natural product residue.

Regarding the reuse capacity of the columns, they could be used more than 40 times with minimum extraction efficiency reduction. In addition, the chromatographic analyses of real jaboticaba peel samples showed the efficiency of the MIP column for catechin extraction and sample cleanup. The developed method presented a potential approach for the extraction of catechin and its derivatives in complex matrices, such as natural product extracts. Compared to traditional offline sample preparation methods, the developed methodology is more eco-friendly, as it presents lower solvent consumption, less laborious processes, and reduced residue production.

## Supplementary Information

Supplementary data are available free of charge at <http://jbcs.sbgq.org.br> as a PDF file.

## Acknowledgments

This research was funded by Coordenação de Aperfeiçoamento de Pessoal de Nível Superior (CAPES) (fellowship program), Conselho Nacional de Desenvolvimento Científico e Tecnológico (CNPq) (grant number 132844/2020-6), and Fundação de Apoio à Pesquisa do Estado de Goiás (FAPEG) (fellowship program).

## Author Contributions

Alessandra T. Cardoso was responsible for conceptualization, methodology, validation, formal analysis, data curation, writing original draft; Rafael O. Martins for writing original draft, methodology, validation; Lucas S. Machado for investigation, visualization; Lucilia Kato for investigation, visualization; Rosineide C. Simas for conceptualization, supervision, resources; Carmen Lúcia Cardoso for investigation, visualization; Andréa R. Chaves for conceptualization, methodology, writing (original draft, review and editing), supervision, project administration. All authors have read and agreed to the published version of the manuscript.

## References

- Motamedi, M.; Yerushalmi, L.; Haghghat, F.; Chen, Z.; *Chemosphere* **2022**, *296*, 133688. [Crossref]
- Martins, N.; Barros, L.; Ferreira, I. C. F. R.; *Trends Food Sci. Technol.* **2016**, *48*, 1. [Crossref]

3. Farajzadeh, M. A.; Nemati, M.; Altunay, N.; Tuzen, M.; Kaya, S.; Kheradmand, F.; Afshar Mogaddam, M. R.; *Microchem. J.* **2022**, *177*, 107291. [Crossref]
4. Torres-Naranjo, M.; Suárez, A.; Gilardoni, G.; Cartuche, L.; Flores, P.; Morocho, V.; *Molecules* **2016**, *21*, 1461. [Crossref]
5. Wang, X.; Li, W.; Gong, Z.; Huang, X.; *Talanta* **2019**, *194*, 7. [Crossref]
6. Tomás-Barberán, F. A.; González-Sarrías, A.; García-Villalba, R.; Núñez-Sánchez, M. A.; Selma, M. V.; García-Conesa, M. T.; Espín, J. C.; *Mol. Nutr. Food Res.* **2017**, *61*, 1500901. [Crossref]
7. Xing, Y.-W.; Wu, Q.-H.; Jiang, Y.; Huang, M.-X.; Lei, G.-T.; *World J. Gastroenterol.* **2019**, *25*, 955. [Crossref]
8. do Nascimento, R. P.; Rizzato, J. S.; Polezi, G.; Moya, A. M. T. M.; Silva, M. F.; Machado, A. P. F.; Franchi Jr., G. C.; Borguini, R. G.; Santiago, M. C. P. A.; Paiotti, A. P. R.; Pereira, J. A.; Martinez, C. A. R.; Marostica Jr., M. R.; *Food Biosci.* **2023**, *53*, 102578. [Crossref]
9. Machado, G. H. A.; Marques, T. R.; de Carvalho, T. C. L.; Duarte, A. C.; de Oliveira, F. C.; Gonçalves, M. C.; Piccoli, R. H.; Corrêa, A. D.; *Chem. Biol. Drug Des.* **2018**, *92*, 1333. [Crossref]
10. Cardullo, N.; Muccilli, V.; Cunsolo, V.; Tringali, C.; *Molecules* **2020**, *25*, 3257. [Crossref]
11. Chupin, L.; Motillon, C.; Charrier-El Bouhtoury, F.; Pizzi, A.; Charrier, B.; *Ind. Crops Prod.* **2013**, *49*, 897. [Crossref]
12. Das, A. K.; Islam, M. N.; Faruk, M. O.; Ashaduzzaman, M.; Dungani, R.; *S. Afr. J. Bot.* **2020**, *135*, 58. [Crossref]
13. Cruz, J. C.; de Souza, I. D.; Lanças, F. M.; Queiroz, M. E. C.; *J. Chromatogr. A* **2022**, *1668*, 462925. [Crossref]
14. Martins, R. O.; Gomes, I. C.; Mendonça Telles, A. D.; Kato, L.; Souza, P. S.; Chaves, A. R.; *J. Chromatogr. A* **2020**, *1620*, 460977. [Crossref]
15. International Conference on Harmonisation (ICH); *ICH Harmonised Tripartite Guideline; Validation of Analytical Procedures: Text and Methodology Q2(R1)*. Retrieved from the International Conference on Harmonisation of Technical Requirements for Registration of Pharmaceuticals for Human Use; ICH: London, 2014.
16. Soares, D. A.; Pereira, I.; Sousa, J. C. P.; Bernardo, R. A.; Simas, R. C.; Vaz, B. G.; Chaves, A. R.; *Food Chem.* **2023**, *400*, 134014. [Crossref]
17. Souza, I. D.; Melo, L. P.; Jardim, I. C. S. F.; Monteiro, J. C. S.; Nakano, A. M. S.; Queiroz, M. E. C.; *Anal. Chim. Acta* **2016**, *932*, 49. [Crossref]
18. Santos, M. G.; Tavares, I. M. C.; Barbosa, A. F.; Bettini, J.; Figueiredo, E. C.; *Talanta* **2017**, *163*, 8. [Crossref]
19. Liu, Q.; Wan, J.; Cao, X.; *Process Biochem.* **2018**, *70*, 168. [Crossref]
20. Trovati, G.; Sanches, E. A.; Neto, S. C.; Mascarenhas, Y. P.; Chierice, G. O.; *J. Appl. Polym. Sci.* **2010**, *115*, 263. [Crossref]
21. Pavia, D. L.; Lampman, G. M.; Kris, G. S.; *Introduction to Spectroscopy*, 5<sup>th</sup> ed.; Cengage Learning: Stamford, 2015.
22. Silveira, J. L. R.; Dib, S. R.; Faria, A. M.; *Anal. Sci.* **2014**, *30*, 285. [Crossref]
23. Abdollah, N. A.; Ahmad, A.; Omar, T. F. T.; *Biointerface Res. Appl. Chem.* **2020**, *11*, 10620. [Crossref]
24. He, S.; Zhang, L.; Bai, S.; Yang, H.; Cui, Z.; Zhang, X.; Li, Y.; *Eur. Polym. J.* **2021**, *143*, 110179. [Crossref]
25. De Middelmeer, G.; Dubruel, P.; De Saeger, S.; *TrAC, Trends Anal. Chem.* **2016**, *76*, 71. [Crossref]
26. Teixeira, L. S.; Silva, C. F.; de Oliveira, H. L.; Dinali, L. A. F.; Nascimento, C. S.; Borges, K. B.; *Microchem. J.* **2020**, *158*, 105252. [Crossref]
27. Guo, L.; Deng, Q.; Fang, G.; Gao, W.; Wang, S.; *J. Chromatogr. A* **2011**, *1218*, 6271. [Crossref]
28. Mejía-Carmona, K.; Lanças, F. M.; *J. Chromatogr. A* **2020**, *1621*, 461089. [Crossref]
29. Soares Maciel, E. V.; de Toffoli, A. L.; da Silva Alves, J.; Lanças, F. M.; *Molecules* **2020**, *25*, 1092. [Crossref]
30. Zenkevich, I. G.; Makarov, A. A.; Pavlovskii, A. A.; *J. Anal. Chem.* **2017**, *72*, 710. [Crossref]
31. Li, P.; Wang, T.; Lei, F.; Peng, X.; Wang, H.; Qin, L.; Jiang, J.; *J. Chromatogr. A* **2017**, *1502*, 30. [Crossref]
32. Martins, G. R.; Guedes, D.; Marques de Paula, U. L.; de Oliveira, M. D. S. P.; Lutterbach, M. T. S.; Reznik, L. Y.; Sérvulo, E. F. C.; Alviano, C. S.; Ribeiro da Silva, A. J.; Alviano, D. S.; *Molecules* **2021**, *26*, 3433. [Crossref]
33. Deflaoui, L.; Setyaningsih, W.; Palma, M.; Mekhoukhe, A.; Tamendjari, A.; *Arab. J. Chem.* **2021**, *14*, 103102. [Crossref]
34. Chaves, J. O.; Sanches, V. L.; Viganó, J.; de Souza Mesquita, L. M.; de Souza, M. C.; da Silva, L. C.; Acunha, T.; Faccioli, L. H.; Rostagno, M. A.; *Food Res. Int.* **2022**, *157*, 111252. [Crossref]
35. Yu, X.; Yu, L.; Ma, F.; Li, P.; *Food Chem.* **2021**, *334*, 127572. [Crossref]
36. Hroboňová, K.; Brokešová, E.; *Food Chem.* **2020**, *332*, 127404. [Crossref]
37. Saad, E. M.; El Gohary, N. A.; Abdel-Halim, M.; Handoussa, H.; Mohamed El Nashar, R.; Mizaikoff, B.; *Food Chem.* **2021**, *335*, 127644. [Crossref]
38. Ersoy, A. K.; Tütem, E.; Başkan, K. S.; Apak, R.; *J. Chromatogr. Sci.* **2020**, *58*, 163. [Crossref]

Submitted: January 10, 2024

Published online: April 23, 2024